RADC-TR-85-233
Final Technical Report
December 1985

RADIATION OF LONG ELECTROMAGNETIC WAVES BY A MODULATED ELECTRON BEAM IN THE IONOSPHERE

Pacific — Sierra Research Corporation

E. C. Field
L. E. Johnson

ROME AIR DEVELOPMENT CENTER
Air Force Systems Command
Griffiss Air Force Base, NY 13441-5700

This report has been reviewed by the RADC Public Affairs Office (PA) and is releasable to the National Technical Information Service (NTIS). At NTIS it will be releasable to the general public, including foreign nations.

RADC-TR-85-233 has been reviewed and is approved for publication.

APPROVED: Dallas T. Hayes

DALLAS T. HAYES
Project Engineer

APPROVED: Allan C. Schell

ALLAN C. SCHELL
Chief, Electromagnetic Sciences Division

FOR THE COMMANDER: John A. Ritz

JOHN A. RITZ
Plans & Programs Division

If your address has changed or if you wish to be removed from the RADC mailing list, or if the addressee is no longer employed by your organization, please notify RADC (EEPS) Hanscom AFB MA 01731. This will assist us in maintaining a current mailing list.

Do not return copies of this report unless contractual obligations or notices on a specific document requires that it be returned.

UNCLASSIFIED
SECURITY CLASSIFICATION OF THIS PAGE

REPORT DOCUMENTATION PAGE

1a. REPORT SECURITY CLASSIFICATION UNCLASSIFIED	1b. RESTRICTIVE MARKINGS N/A
2a. SECURITY CLASSIFICATION AUTHORITY N/A	3. DISTRIBUTION / AVAILABILITY OF REPORT Approved for public release; distribution unlimited.
2b. DECLASSIFICATION / DOWNGRADING SCHEDULE N/A	
4. PERFORMING ORGANIZATION REPORT NUMBER(S) PSR Report 1566	5. MONITORING ORGANIZATION REPORT NUMBER(S) RADC-TR-85-233
6a. NAME OF PERFORMING ORGANIZATION Pacific-Sierra Research Corp 6b. OFFICE SYMBOL (If applicable)	7a. NAME OF MONITORING ORGANIZATION Rome Air Development Center (EEPS)
6c. ADDRESS (City, State, and ZIP Code) 12340 Santa Monica Boulevard Los Angeles CA 90025	7b. ADDRESS (City, State, and ZIP Code) Hanscom AFB MA 01731
8a. NAME OF FUNDING / SPONSORING ORGANIZATION Rome Air Development Center 8b. OFFICE SYMBOL (If applicable) EEPS	9. PROCUREMENT INSTRUMENT IDENTIFICATION NUMBER F19628-84-C-0014
8c. ADDRESS (City, State, and ZIP Code) Hanscom AFB MA 01731	10. SOURCE OF FUNDING NUMBERS PROGRAM ELEMENT NO. 61102F; PROJECT NO. 2305; TASK NO. J2; WORK UNIT ACCESSION NO. 46

11. TITLE (Include Security Classification)
RADIATION OF LONG ELECTROMAGNETIC WAVES BY A MODULATED ELECTRON BEAM IN THE IONOSPHERE

12. PERSONAL AUTHOR(S)
E. C. Field, L. E. Johnson

13a. TYPE OF REPORT	13b. TIME COVERED	14. DATE OF REPORT (Year, Month, Day)	15. PAGE COUNT
Final	FROM Dec 83 TO Aug 85	December 1985	48

16. SUPPLEMENTARY NOTATION
N/A

17. COSATI CODES		
FIELD	GROUP	SUB-GROUP
20	14	
17	02	

18. SUBJECT TERMS (Continue on reverse if necessary and identify by block number)
Cerenkov Radiation
ELF
Long Wavelength Communication
Low-Frequency Communications
Modulated Electron Beams
(See Reverse)

19. ABSTRACT (Continue on reverse if necessary and identify by block number)

Pulsed electron beams in the ionosphere radiate electromagnetic energy and, therefore, might work as wireless virtual antennas. Such virtual antennas would be most useful at low frequencies because small or moderate-size wire antennas work well at high frequencies. Natural beams radiate energy that propagates down through the ionosphere, but no experiment has used a man-made electron beam to produce radiation at the modulation frequency or its harmonics, and detected that radiation on the ground. The present report addresses the feasibility of such an experiment, and suggests preferred configurations. Motivated by communications applications, which require good time availability, it considers only phenomena, such as the triggering plasma of instabilities or guidance in transient ionospheric ducts.

A 1 keV 30 kW beam will radiate several kilowatts into the Cerenkov mode, provided the frequency exceeds a few kilohertz and the beam retains its coherence for at least tens

20. DISTRIBUTION / AVAILABILITY OF ABSTRACT	21. ABSTRACT SECURITY CLASSIFICATION
☒ UNCLASSIFIED/UNLIMITED ☐ SAME AS RPT ☐ DTIC USERS	UNCLASSIFIED
22a. NAME OF RESPONSIBLE INDIVIDUAL Dr. Dallas T. Hayes	22b. TELEPHONE (Include Area Code) (617) 861-4264 22c. OFFICE SYMBOL RADC (EEPS)

DD FORM 1473, 84 MAR 83 APR edition may be used until exhausted. All other editions are obsolete.

SECURITY CLASSIFICATION OF THIS PAGE
UNCLASSIFIED

of meters. A 10 keV beam might also radiate well, but would have to retain coherence over distances of hundreds to thousands of meters. The radiation is detectable at the ground, provided detection bandwidths less than about 100 Hz are achieved by coherently summing the output of tens to hundreds of beam pulses.

The beam should be injected at altitudes up to 400 km. The necessary electron gun and power supply are not yet developed, but would use near-term technology and could be carried aloft by a rocket or the shuttle. The interaction of the beam with the ionospheric plasma could be monitored by instruments on diagnostics packages. More theoretical work is needed to relax idealizations inherent in currently used beam/propagation models.

18. SUBJECT TERMS (Continued)

Virtual Antennas
VLF

TABLE OF CONTENTS

LIST OF FIGURES

I. INTRODUCTION

Early studies of space-based long-wave transmitters were motivated by the hope that an antenna in the ionosphere might be smaller and more efficient than its counterpart below the ionosphere. That hope was based on three facts: first, waves in the ionosphere are shorter than in free space; second, guidance in ionospheric ducts or along geomagnetic field lines sometimes focuses the signal, thereby enhancing antenna gain; and, third, plasma instabilities sometime amplify long-wave signals, such as whistlers. Many of the original papers on space-based wire antennas are contained in the Proceedings of the Conference on ELF/VLF Downlink Satellite Communications [1]. Despite that early enthusiasm, technological and funding constraints have prevented realization of a practical space-based long-wave antenna, although experiments using wire antennas a hundred kilometers or more long have been designed recently [2].

Pulsed electron beams in the ionosphere radiate electromagnetic energy and, therefore, might work as wireless virtual antennas [3,4,5,6]. Such virtual antennas are most needed at frequencies below a megahertz, because small or moderate-size wire antennas work well at higher frequencies. Natural beams often radiate energy that propagates down through the ionosphere, but no experiment has been performed in which a man-made electron beam produced radiation at the modulation frequency or its harmonics that has been detected on the ground. The present report addresses the feasibility of such an experiment, and suggests preferred configurations.

This report relies heavily on the results of an earlier study by Johnson [7] that uses the linear theory of Harker and Banks [3, 4] to predict radiation for various beam parameters. It shows that the radiation efficiency typically is either low or high, but seldom moderate. Combinations of beam energy, current, modulation frequency, and altitude that give low efficiencies guarantee failure and should be avoided. Conversely, parameter combinations that give high calcu-

lated efficiencies should be used. They do not, however, guarantee success, because the linear theory, accurate for weakly radiating beams, overstates the efficiency of strongly radiating ones. Our approach, therefore, is to define parameter combinations that are necessary for a successful experiment, but which--although encouraging--cannot at this time be proven sufficient.

Because it is motivated by possible communications applications, which require high time availability, this report omits sporadic phenomena such as the triggering of plasma instabilities or guidance in transient ionospheric ducts.

II. BACKGROUND

In this section we briefly review, first, the mechanisms by which pulsed electron beams radiate electromagnetic energy and, second, prior experiments on beams in the ionosphere.

HOW BEAMS RADIATE

An electron beam in the ionosphere produces electromagnetic and electrostatic waves. Being longitudinal, electrostatic waves have no magnetic field and cannot exist in free space. They therefore couple poorly to the neutral atmosphere and would probably not give rise to a signal detectable at the ground. For that reason, this report considers only electromagnetic waves.

The two main types of electromagnetic radiation produced by stable electron beams are: (1) synchrotron radiation at the Doppler-shifted gyrofrequency and its harmonics, and (2) Cerenkov radiation. Because the electron gyrofrequency is about a 1 MHz, Cerenkov radiation is the more important mechanism for generating long, low frequency waves. It occurs even if the beam moves in a straight line at constant speed, because ionospheric charged particles are accelerated by the electric field carried by the beam's electrons and radiate electromagnetic energy. If the beam is pulsed, the radiation will be periodic at the pulse repetition--or modulation--frequency.

Only if the beam velocity exceeds the phase velocity in the ionosphere can the Cerenkov wavelets interfere constructively and form a coherent wavefront. Even then, coherent radiation occurs only in preferred directions. When the propagation is isotropic, the wavefronts are cones of half-angle $\arcsin(c/\mu v)$, where c is the vacuum speed of light, v is the beam velocity, and μ is the refractive index, which must exceed unity for Cerenkov radiation to occur. That Cerenkov cone is analogous to the familiar Mach cone that bounds the wake of a supersonic body.

The phase velocity of long waves in the ionosphere is a small

fraction of the vacuum light speed. Beams of modest energy can therefore produce Cerenkov radiation, although the situation in the anisotropic ionosphere is more complicated than described above for isotropic media. The geomagnetic field--without which the slow waves of interest could not exist--causes the phase velocity to depend on direction and frequency. However, if the beam is directed along the geomagnetic field, the Cerenkov wavefronts are still cones symmetric about the beam's axis, as diagrammed by Fig. 1. Phase considerations show that the beam velocity must equal that of the cone apex along a magnetic field line.

Beams not directed along the geomagnetic field trace helices and the wavefronts then depend in a complicated way on frequency and direction, as well as on the beam's pitch angle. The radial acceleration produces synchrotron radiation--often called cyclotron modes. As mentioned, cyclotron modes tend to be less important than Cerenkov radiation at the frequencies of interest here.

PREVIOUS EXPERIMENTS

Energetic electrons of natural origin are well-known to produce Cerenkov radiation in the ionosphere, having been suggested as a source of very-low-frequency (VLF) hiss nearly 30 years ago [8]. Here, however, we concentrate on experiments that used rocket- and satellite-borne electron guns as probes to better understand auroral physics, beam-plasma interactions, and wave generation (e.g., Winkler, [9]). In planning those early experiments, it was feared that two-stream instabilities or vehicle charge-up would severely limit the length and current of beams injected into the ionosphere. Degradation from those effects proved much less catastrophic than anticipated, however. Beams have traveled 100 km or more [10] and there is evidence that they have made a total round-trip of 38 earth radii to and from the point conjugate to the place of injection [9].

Two mechanisms mitigate vehicle charging. First, the charging vehicle accelerates nearby ionospheric electrons, which collide with neutral molecules and atoms and produce secondary electrons. Those

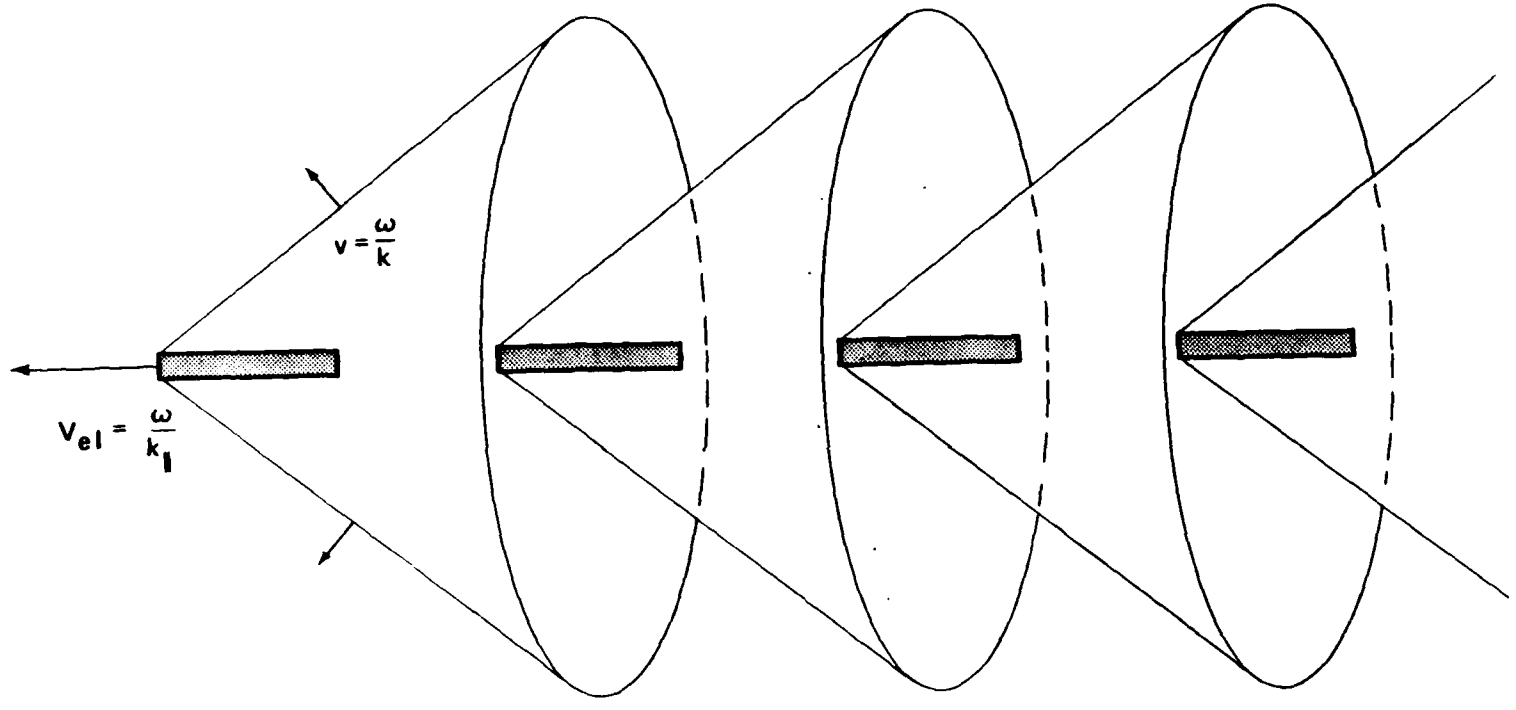

Figure 1. Cerenkov wavefronts radiated by infinite train of electron pulses in ionosphere.

secondaries surround and neutralize the vehicle. The second mechanism is beam-plasma discharge, where electrons streaming toward the positively charged vehicle set up high-frequency electrostatic fields in the surrounding plasma. Those fields accelerate plasma electrons, which ionize the much more numerous neutral particles, thereby producing additional electrons to cancel the vehicle's positive charge. Calculations show that those two mechanisms limit the potential of a vehicle with a 0.5-A beam to less than 100 V, in accordance with measurements.

Many of the 25 or so missions that used electron beams deployed electromagnetic detectors near the vehicle or the beam. Electromagnetic waves were detected near the plasma frequency (about 10 MHz), twice the electron cyclotron frequency (a few megahertz), in the whistler band (below a few hundred kilohertz), at the beam modulation frequency 3 kHz) and, in some cases, not at all (e.g., [11, 12, 13]). All those measurements were made at short ranges, well within a wavelength from the source. It is therefore impossible to tell whether much energy was actually radiated, or the fields were predominantly nonradiative near fields. Measurements at greater distances are needed to determine radiation efficiencies.

Radiation from ionospheric beams has been detected on the ground at frequencies above those of interest here. High-frequency emissions were detected during the Zarnitza, ARAKS, and Echo V flights [9]. Their origin is uncertain, but possible generation mechanisms include acceleration of electrons in the sheath around the rocket or in the ionized region surrounding the beam. Synchrotron radiation at 2.96 MHz, twice the cyclotron frequency, reached the ground during the Echo IV experiment.

In summary, near fields of beams have been detected at frequencies below a 1 MHz, and radiation fields have been detected on the ground at frequencies above a 1 MHz. No experiment has yet modulated a beam at low frequencies and measured radiation fields at the modulation frequency or its harmonics.

III. THRESHOLDS ON POWER, GAIN, AND BANDWIDTH

In this section we estimate the power that must be radiated by a source in the ionosphere to produce a signal that is detectable on the ground. That threshold power pertains to any source--beam or conventional antenna--and depends on directional gain, bandwidth, and certain geophysical parameters. In Sec. IV we calculate power radiated by modulated beams and compare that power to the threshold for a successful experiment.

We assume, conservatively, that the signal power density must exceed the noise power density by a factor of 10 (10 dB) to ensure detection. Because long-wave receivers are usually atmospheric-noise-limited, that criterion is

$$\frac{PGA}{4\pi R^2} \geq 10NW \quad \text{watts/m}^2 , \tag{1}$$

where P is the radiated power, G is the gain, A is the fraction of the downward-propagating signal not absorbed in the ionosphere, R is the distance from source to receiver, N is the atmospheric noise density, and W is the bandwidth of the received signal. The threshold power P_T that must be radiated for reliable detection on the ground is therefore

$$P_T = \left(\frac{40\pi R^2 N}{A}\right)\left(\frac{W}{G}\right) \quad \text{watts} . \tag{2}$$

The quantity in the first bracket on the right-hand side of Eq. (2) depends solely on geophysical parameters; the one in the second bracket depends on the source and receiver.

Of the geophysical parameters, the most difficult to quantify is the transmission factor A. We use simple estimates by Booker, Crain, and Field [14], who present graphs of one-way transionospheric absorp-

tion. However, a detailed analysis of the excitation of the earth-ionosphere waveguide is needed to determine accurately the "footprint" of a downward-propagating wave.

Table 1 gives the values assumed for the transmission factor A and the atmospheric noise density N. We assume nighttime conditions, because transionospheric absorption is lower at night than in the daytime. The values for N are taken from Watt [15], Watt and Maxwell [16], and Evans and Griffiths [17]. Note the minimum in VLF noise that occurs at around 3 kHz.

TABLE 1. Nighttime Values for Atmospheric Noise Density and Transionospheric Transmission Coefficient.

Frequency, F (kHz)	N (W/m^2-Hz)	A
0.1	10^{-11}	0.3
1	1.5×10^{-11}	0.3
3	5×10^{-12}	0.3
10	2.5×10^{-11}	0.3
30	8×10^{-12}	0.25
100	8×10^{-14}	0.2

The parameters in Table 1 are used with Eq. (2) to express the threshold power in terms of bandwidth and directional gain, once a range R is selected. Although bandwidth is a useful parameter, it is helpful also to express the threshold power P_T in terms of the coherent integration time τ and the number M of pulses that must be summed coherently to achieve the bandwidth W. The following approximate relations define the transformations to apply to Eq. (2), where F is the carrier frequency:

$$W = \frac{1}{\tau} = \frac{F}{M} \quad \text{Hz} . \tag{3}$$

Table 2 shows the threshold power, expressed in kilowatts, for a range of 300 km, which represents a nominal altitude for a rocket-borne electron gun. That table gives the thresholds in terms of directional gain G, bandwidth W (in hertz), integration time τ (in seconds), and number of pulses coherently summed M. Values of P_T for other altitudes are obtained easily by noting the proportionality to R^2 given in Eq. (2).

TABLE 2. Threshold Radiated Power for Reception on Ground.

Frequency (kHz)	Threshold Power, P_T (kw)		
0.1	0.4 W/G	$0.4/G\tau$	40/MG
1	0.6 W/G	$0.6/G\tau$	600/MG
3	0.2 W/G	$0.2/G\tau$	600/MG
10	1 W/G	$1/G\tau$	10^4/MG
30	0.4 W/G	$0.4/G\tau$	1.2×10^4/MG
100	0.005 W/G	$0.005/G\tau$	500/MG

It is difficult to specify an upper limit on the power that could be input to an electron beam in space, but 30 kW seems a realistic expectation for the near future. It is unlikely that more than 20 percent of that energy could be radiated without disrupting the beam's trajectory and waveform. Therefore, we use 5 kW as a working number for the maximum power that could be radiated. More specifically, an experiment is probably impractical if the threshold power P_T shown in Table 2 substantially exceeds 5 kW, but--subject to the analysis in Sec. IV--is feasible if P_T is below 5 kW.

The third column in Table 2 indicates that the product MG of the number of pulses summed and the directional gain must be large for energy radiated into the ionosphere to be detected on the ground. The well-known formula for directional gain is

$$G = \frac{27{,}000}{\theta^2} , \tag{4}$$

where θ is the half-power angular width of the radiation pattern in degrees. Analysis given in [7] shows that the radiation patterns range from broad to very narrow, with the narrowest occurring at the highest frequencies. Unfortunately, experience with whistlers shows that even when the radiation pattern at the source is narrow, refractive spreading--particularly at the base of the ionosphere--causes 10 deg or more divergence. The gain realized on a long-wave ionosphere-to-ground link will thus seldom exceed 100.

Therefore, depending on frequency and the gain actually achieved, a successful experiment requires coherent summation of the energy radiated from tens to hundreds of beam pulses.

IV. RADIATION FROM MODULATED ELECTRON BEAMS IN IONOSPHERE

All existing theories synthesize the radiation by an electron beam, modulated or unmodulated, from the radiation by a single electron moving in a path unperturbed by a surrounding ambient plasma [3, 18, 19, 20, 6, 5]. Such linear theories neglect interactions between the beam and plasma, including: beam slowing from radiative energy loss; beam disruption by plasma instabilities or beam-plasma discharge; beam cancellation by return currents; and alteration of the surrounding plasma by ionization or formation of sheaths. The present report uses the method of Harker and Banks [4] which, in addition to the idealizations just mentioned, assumes the beam to be so long and narrow that the electron gyroradius and the beam's width and angular spread are negligibly small.

Most of those neglected phenomena would, if accounted for, reduce the beam's radiation efficiency. The theory therefore overstates the radiation, and that overstatement is greatest for parameters that lead to strong radiation and, hence, nonlinear effects. Because the theory provides an upper bound, we interpret its results as follows: parameters for which the predicted radiation is inadequate will lead to a failed experiment and should be avoided; parameters for which the predicted radiation is more than adequate are encouraging and should be used in experiments, although success is not guaranteed.

CALCULATED RADIATION

Figures 2 and 3 are examples of the extensive results presented in [7] and show contours of nighttime Cerenkov radiation rates at the fundamental frequency of a square-wave-modulated beam for altitudes of 200 km and 400 km. The assumed input power--the product of beam energy and current--is 30 kW; conversion to other input powers is made by using the proportionality of the radiated power to the square of the current. Because the calculated radiation is proportional to beam length, the contours are labeled with the logarithm of the number of watts radiated per meter of beam; the contour labeled "2.0" cor-

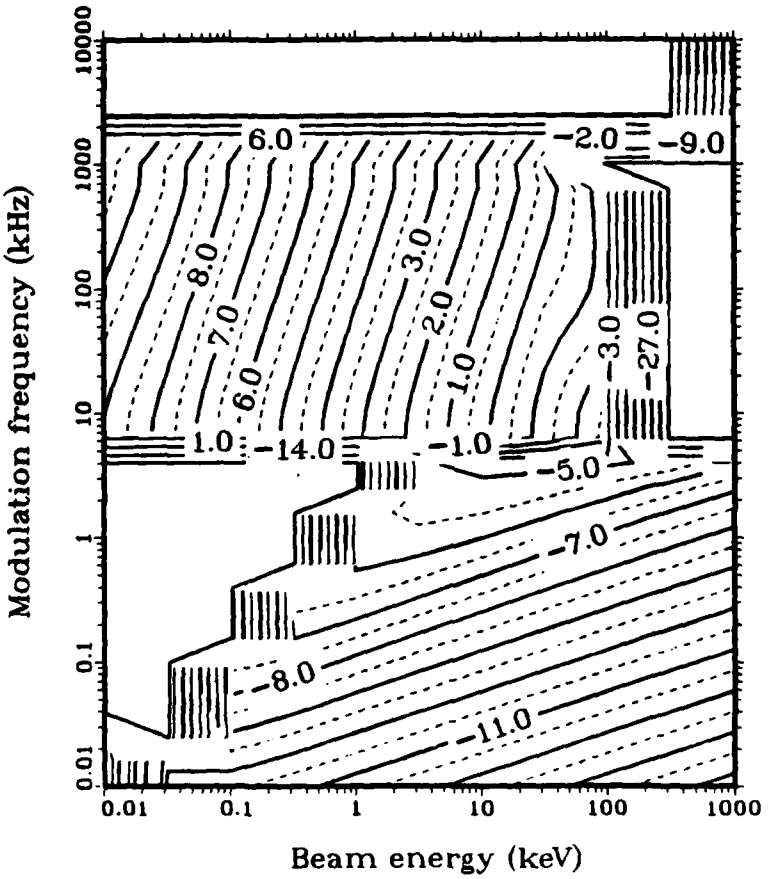

Figure 2. Nighttime Cerenkov radiation rate (watts per meter of beam) contour: 200 km altitude; 30 kW beam; 45 deg pitch angle; midlatitude.

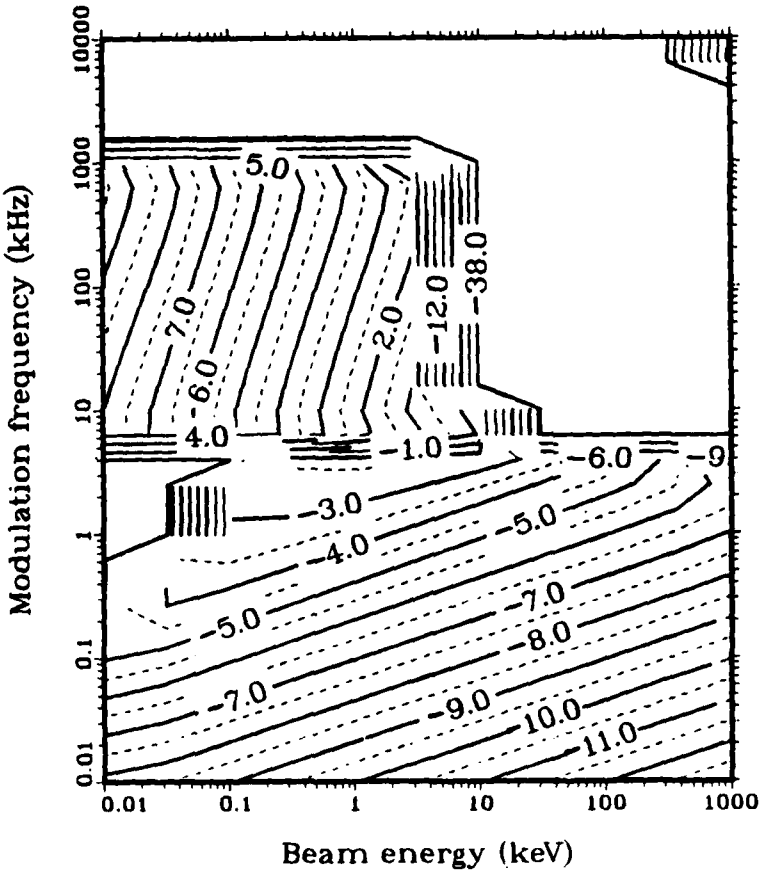

Figure 3. Nighttime Cerenkov radiation rate (watts per meter of beam) contour: 400 km altitude; 30 kW beam; 45 deg pitch angle; midlatitude.

responds to 100 W/m, and the contour labeled "-1.0" corresponds to 0.1 W/m, for example. The reader should check the contour labels carefully for the minus signs. For ease of presentation, the figures show results for beam energies between 0.01 and 1000 keV. However, our nonrelativistic theory is inaccurate above a few hundred keV. And, at least for 30 kW input power, beam energies below a few tenths of an electronvolt correspond to currents that could exceed practical limits.

The figures show the importance of selecting proper combinations of modulation frequency and beam energy. The radiation is intense for certain combinations, weak for others. Moreover, there exist forbidden zones, shown as blank regions in Figs. 2 and 3, where wave and particle velocities cannot satisfy resonant conditions given in [7] and, hence, the beam cannot radiate.

Figures 4 and 5 replot data from Fig. 3 in two-dimensional format. Figure 4 shows the radiation versus modulation frequency for various beam energies; Fig. 5 shows it versus energy for various frequencies. Frequencies above a few kilohertz are clearly preferred, and, subject to that frequency constraint, low energies work better than high ones. That conclusion cannot be pushed to extremes, however. As mentioned, very low energies correspond to currents greater than about 100 A, which could exceed the capabilities of practical space-borne electron guns.

BEAM RADIATION LENGTH (BRL)

The beam radiation length--defined as the distance over which the beam must hold together in order to radiate 20 percent of its input power into the Cerenkov mode--is a convenient parameter that characterizes the beam's radiation efficiency. A short radiation length is desirable, because it implies the beam will radiate much of its energy before various phenomena disrupt its coherence. Long radiation lengths, on the other hand, are discouraging, because the beam might be disrupted before being able to radiate effectively. Our choice of 20 per cent radiation as the definition of the radiation length is

somewhat arbitrary, but reasonable: 20 per cent is about as much energy as a beam could lose to radiation without slowing down substantially. This point is elaborated below.

By definition, the beam radiation length BRL is given by

$$BRL = 0.2P/p = 0.2EI/p \quad \text{meters}, \tag{5}$$

where P is the input power, I is the beam current, E is the beam energy, and p is the power radiated per meter of beam length shown in Figs. 2 through 5. Table 3 shows the beam radiation length and other parameters, discussed below, for nighttime conditions and the assumed input power P of 30,000 W.

CHARACTERISTIC LENGTHS

Table 3 gives a number of characteristic lengths that are useful for interpreting and verifying certain approximations. The following paragraphs give formulas for those lengths and discuss their significance.

(A) Mean Forward Range (MFR)

The mean forward range path is the distance traveled by a beam electron before it is stopped by collisions with neutral particles. If the MFR is much greater than the radiation length, collisions will not disrupt the beam before it can radiate; if it is smaller, collisions could destroy the beam's ability to radiate. The formula for the mean forward range is simply

$$MFR = 4.12 \times 10^{-3} E^{(1.265 - 0.0954 \ln E)/\rho} \quad \text{meters}, \tag{6}$$

a. Lower powers.

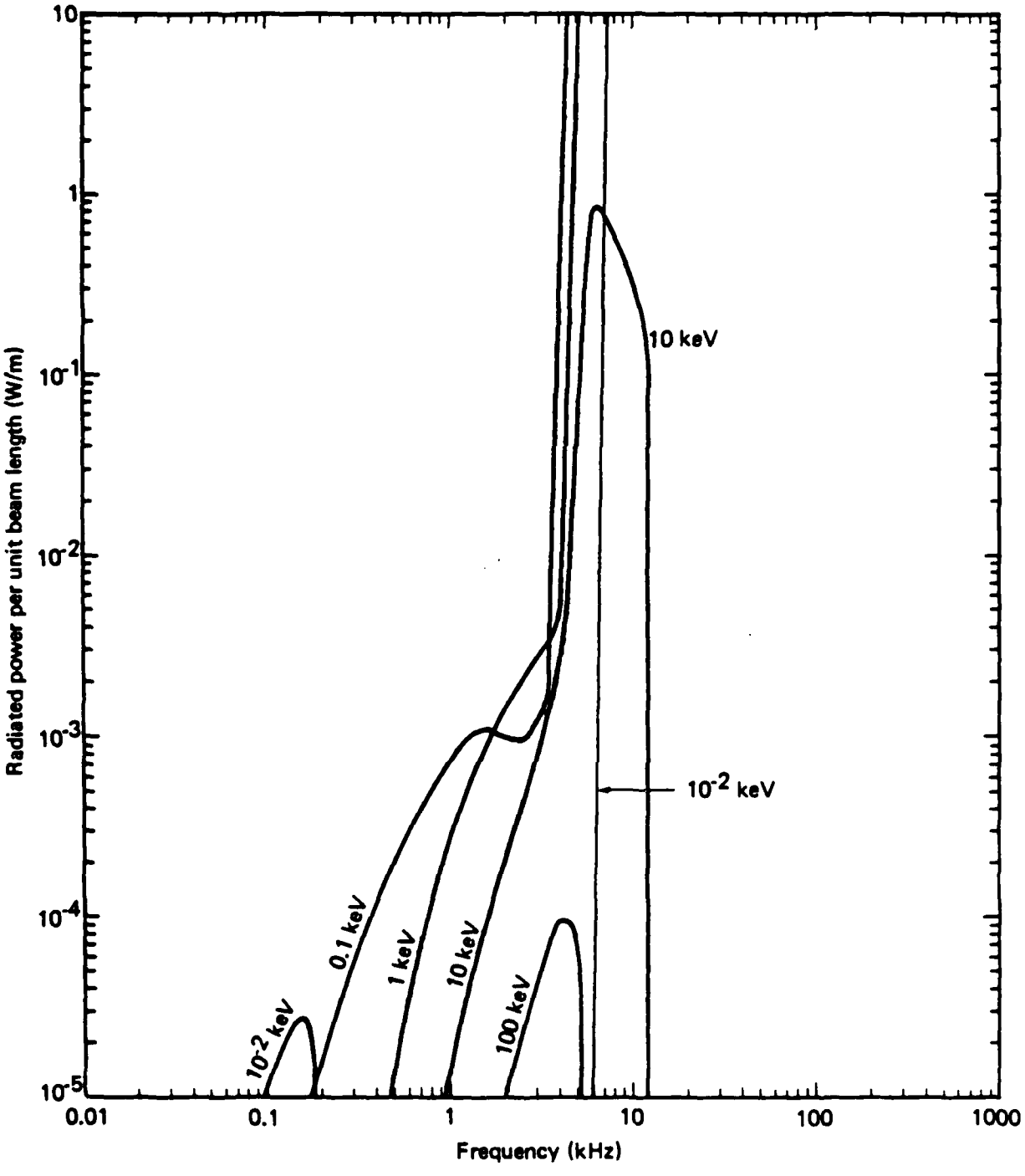

Figure 4. Radiation rate versus modulation frequency for various beam energies: 400 km altitude; 30 kW beam; 45 deg pitch angle; midlatitude.

b. Higher powers.

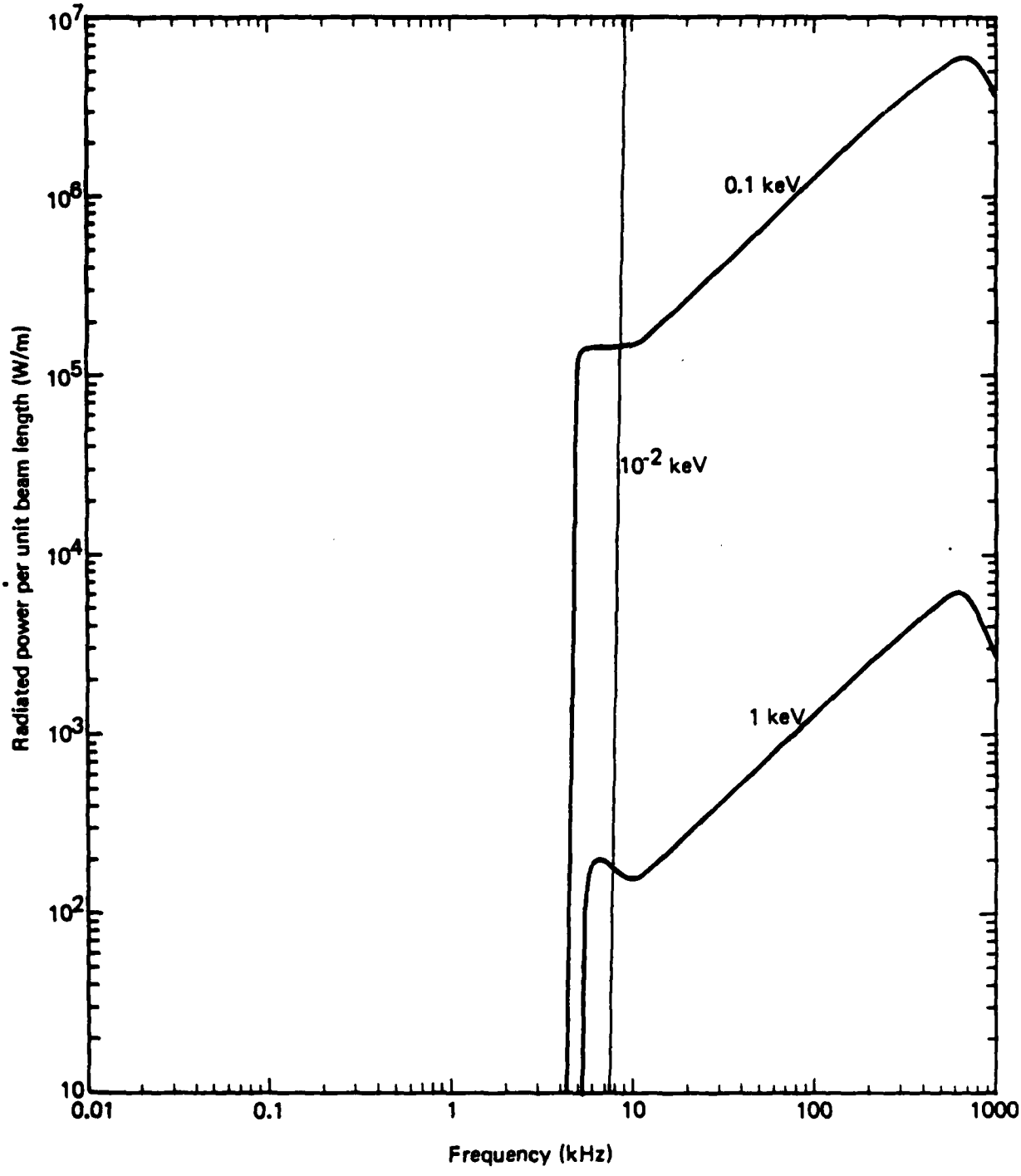

Figure 4. Continued.

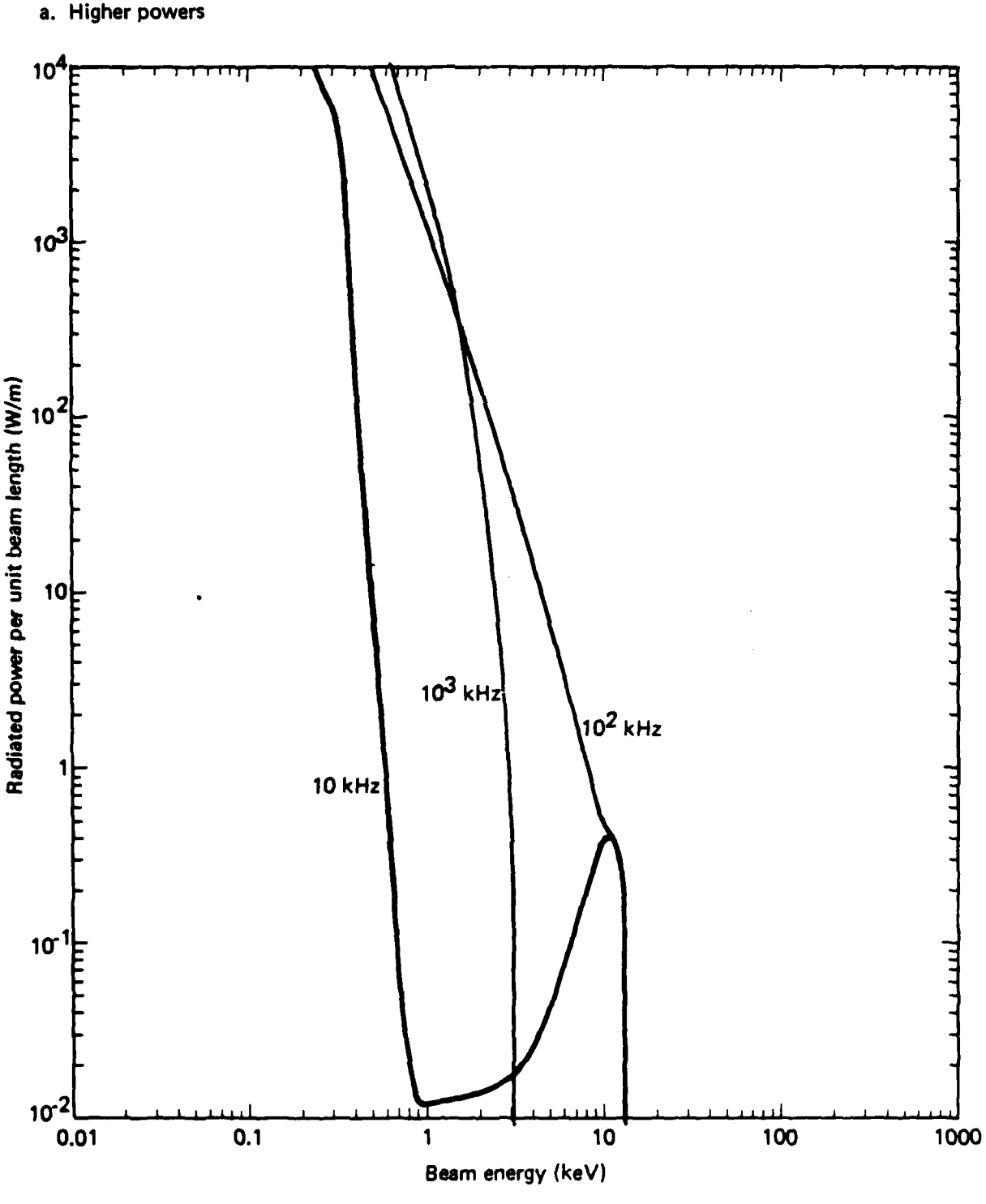

Figure 5. Radiation rate versus beam energy for various frequencies: 400 km altitude; 30 kW beam; 45 deg pitch angle; midlatitude.

b. Lower powers.

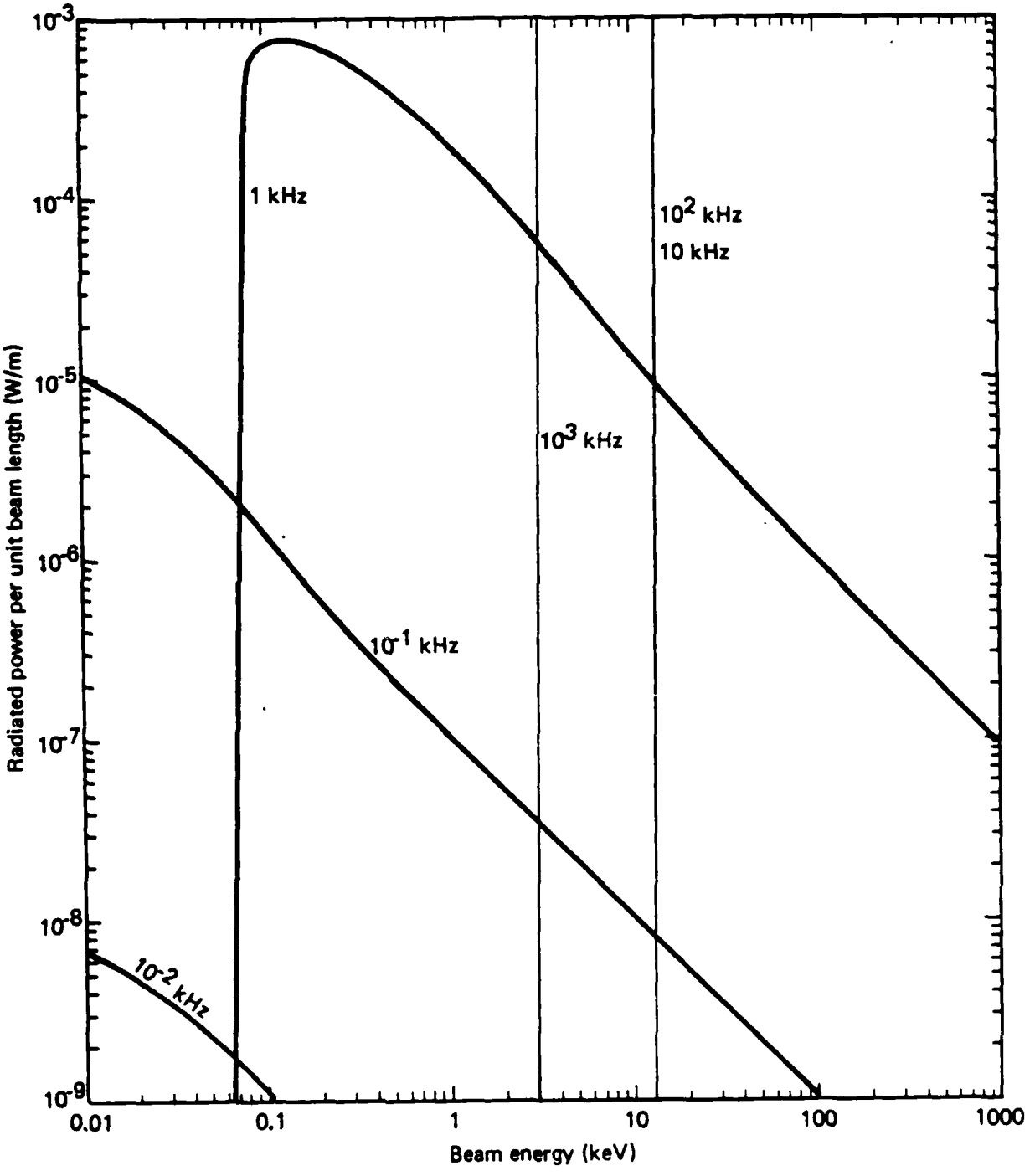

Figure 5. Continued.

TABLE 3. Characteristic Lengths (in Meters).

Altitude (km)	Beam Energy (keV)	Mean Forward Range (MFR)	Beam Plasma Discharge Length (BPDL)	Brillouin Radius (RB)	Larmor Radius (R_L)	Frequency (F)	Free Space Wavelength (λ_0)	Wavelength in Ionosphere (λ)	Long Beam Criterion (L_0)	Beam Radiation Length (BRL)
200	1	2.7×10^4	8.5×10^{-2}	22	1.7	1	3×10^5	6.9×10^3	750	2.6×10^9
						10	3×10^4	14.1	3×10^{-3}	3.4
						100	3×10^3	16.1	4×10^{-3}	0.2
	10	6.3×10^6	27	4	5.4	1	3×10^5	2.8×10^3	195	6×10^4
						10	3×10^4	45	0.3	3.4×10^3
						100	3×10^3	52	0.1	4×10^2
300	1	3.3×10^5	0.8	23	1.8	1	3×10^5	700	170	3.6×10^7
						10	3×10^4	9.1	51	32
						100	3×10^3	14.7	61	3.6
	10	7.7×10^7	235	4.1	5.7	1	3×10^5	530	160	6×10^8
						10	3×10^4	37	20	2×10^5
						100	3×10^3	61	4	6×10^3
400	1	1.9×10^6	3.8	24	1.9	1	3×10^5	620	46	2.8×10^4
						10	3×10^4	9.8	2.5×10^{-2}	38
						100	3×10^3	12.7	4.1×10^{-2}	4.4
	10	4.4×10^8	1200	4.2	5.9	1	3×10^5	463	2.2	6×10^8
						10	3×10^4	47.5	0.47	6×10^8
						100	3×10^3	--	--	--

where E is the beam energy in MeV and ρ is the neutral density in grams per centimeter squared. Table 2 shows the MFR to be several hundred kilometers or more.

(B) Beam-Plasma Discharge Length (BPDL)

Beam-plasma discharge (BPD) appears at a critical length, given approximately by

$$BPDL = 3 \times 10^{-11} E^{2.5}/B^{0.7}\psi P \quad \text{meters}, \tag{7}$$

where the beam energy is in volts, the earth's magnetic field B is in Gauss, and the atmospheric pressure ψ is in torr. To derive Eq. (7) we inserted $I = P/E$ into a formula for critical current given by Szuszczewicz [21].

Once established, BPD causes production of ion pairs, optical emission, high-frequency wave emission, and modification of the primary beam velocity. The last effect is of concern, because changing the beam's velocity might alter its ability to radiate. Most observations of BPD have occurred in laboratory plasmas, although an observation has recently been made in space [22]. Neither the extent to which BPD occurs in space plasmas, nor the extent to which it disrupts the beam, are well known. As mentioned, BPD seems less disruptive to space beams than originally feared, but more data are needed.

Calculated values of the BPDL, shown in Table 3, range from around a meter up to several hundred meters--shorter than the beam radiation length. Therefore, although BPD has apparently not seriously affected space beams, it could, if operative, prevent a beam from attaining the length needed for maximum radiation.

(C) Brillouin Radius (BR)

In contrast to Harker and Banks' assumption of a filamentary beam, Lavergnat, Lehner, and Matthieussent [5] assume the beam to expand until its radius equals the Brillouin radius, which arises from the balancing of the Lorentz and repulsive forces situation and is given by

$$RB = \left[\frac{eI}{2\pi\varepsilon_o V_{||} m\omega_b^2}\right]^{1/2} \quad \text{meters,} \qquad (8),$$

where e is the electron charge, $V_{||}$ is the component of beam velocity parallel to the geomagnetic field, m is the electron mass, ε_o is the free-space permittivity, and ω_b is half the angular gyrofrequency in radians per second.

The Brillouin radius is an idealized mathematical solution for equilibrium beam flow in a vacuum, so its relevance to beams in space plasmas is uncertain. Moreover, the angular divergence--at least a few degrees--that most beams have upon leaving the electron gun probably is the main cause of beam spreading. Nonetheless, the beam radius will surely be no smaller than the Brillouin radius. And, our assumption of a filamentary beam is therefore violated if the beam's length does not exceed that radius by a substantial amount.

Table 2 shows the Brillouin radius to be a few meters for a 1 KeV beam, and about 20 m for a 10 KeV beam.

(D) Larmor Radius (R_c)

The radiation per unit length shown in Figs. 3 through 6 is averaged over many cyclotron periods. That procedure is valid only if the beam is much longer than the Larmor radius. We do not repeat the well-known formula for the Larmor radius here, but show numerical values in Table 3 for a beam pitch angle of 45 deg. Those values are typically a few meters.

(E) Wavelength in Ionosphere (λ)

The wavelength in the ionosphere is given by

$$\lambda = c/F\mu \quad \text{meters}, \tag{9}$$

where c is the vacuum speed of light, F is the modulation frequency, and μ is the refractive index in the direction of propagation. Note that μ depends strongly on direction, and the radiation is typically emitted over a narrow angular range, so μ can be calculated only after a complicated determination of the radiation direction. Details are given in Johnson [7] and in Harker and Banks [4], and numerical values for local wavelength shown in Table 3.

Because the local wavelengths are much shorter than the free space ones, the near-field zone in the ionosphere is much smaller than in free space. That fact is important for ascertaining how far a diagnostic package must be separated from the beam to measure the radiation fields.

A word of caution: the local wavelengths shown in Table 3 apply only in a narrow conical region where certain resonant conditions are met and the refractive index μ is large; in other directions, the local wavelengths are somewhat longer than shown, but still much shorter than in free space.

(F) Long-Beam Criterion (L_o)

The graphs in Figs. 3 through 5 were calculated using the long-beam approximation. The complicated formula for L_o, the beamlength that must be exceeded for that theory to be strictly valid, is given by Harker and Banks [4]; Table 3 gives numerical values. When the radiation length BRL exceeds L_o, the calculation is self-consistent; otherwise it is not, because the theory predicts the beam radiates most of its initial energy before reaching long-beam status. The best interpretation of the latter case is that the beam indeed radiates strongly, although the calculated values might be imprecise. Sample

calculations, not given in detail here, show that the short-beam regime overlaps the long-beam regime.The results in Table 3 are, therefore, meaningful even when BRL is somewhat shorter than L_o.

BEAM SLOWDOWN

Comparison of the beam radiation length with the other lengths given in Table 3 shows that, in certain regimes, the linear theory predicts that beam slowdown is dominated by energy loss to radiation. As the beam slows, its energy and current decrease, and its radiation efficiency changes. A rigorous treatment of beam slowing would require inclusion of the nonlinear braking effect of the Cerenkov fields on the beam. Instead, within the framework of the linear theory, we perform a heuristic calculation that approximates beam slowing in a stepwise fashion. Specifically, starting with the radiated power density at the gun, we calculate the power radiated in a given increment of beam length, adjust the beam energy accordingly, and compute a new radiated power density for the next increment. The steps are repeated until all the electron energy is lost to radiation.

As an illustration, we have analyzed the effect of beam slowing at an operating point chosen for high radiation efficiency: modulation frequency 40 kHz, initial beam energy 3 kV, pitch angle 45 deg, and gun output 30 kW. For this case, the linear theory states that for a beam emitted at 400 km altitude the radiated power per meter beam length is 18.5 W.

Figure 6 shows the results of the stepwise linear calculation. If the radiated power remained constant as the beam slowed, the beam power would be dissipated in about 1.6 km. In fact, the radiated power does remain nearly constant for a few hundred meters. But the radiation efficiency increases as the beam loses energy, so the radiated power increases sharply during the final few hundred meters, where the current and energy drop rapidly. At 1.1 km from the gun, the beam has lost practically all its energy.

The same analysis shows that radiation's ray and phase angles change by only a few hundredths of a degree as the beam slows. Thus,

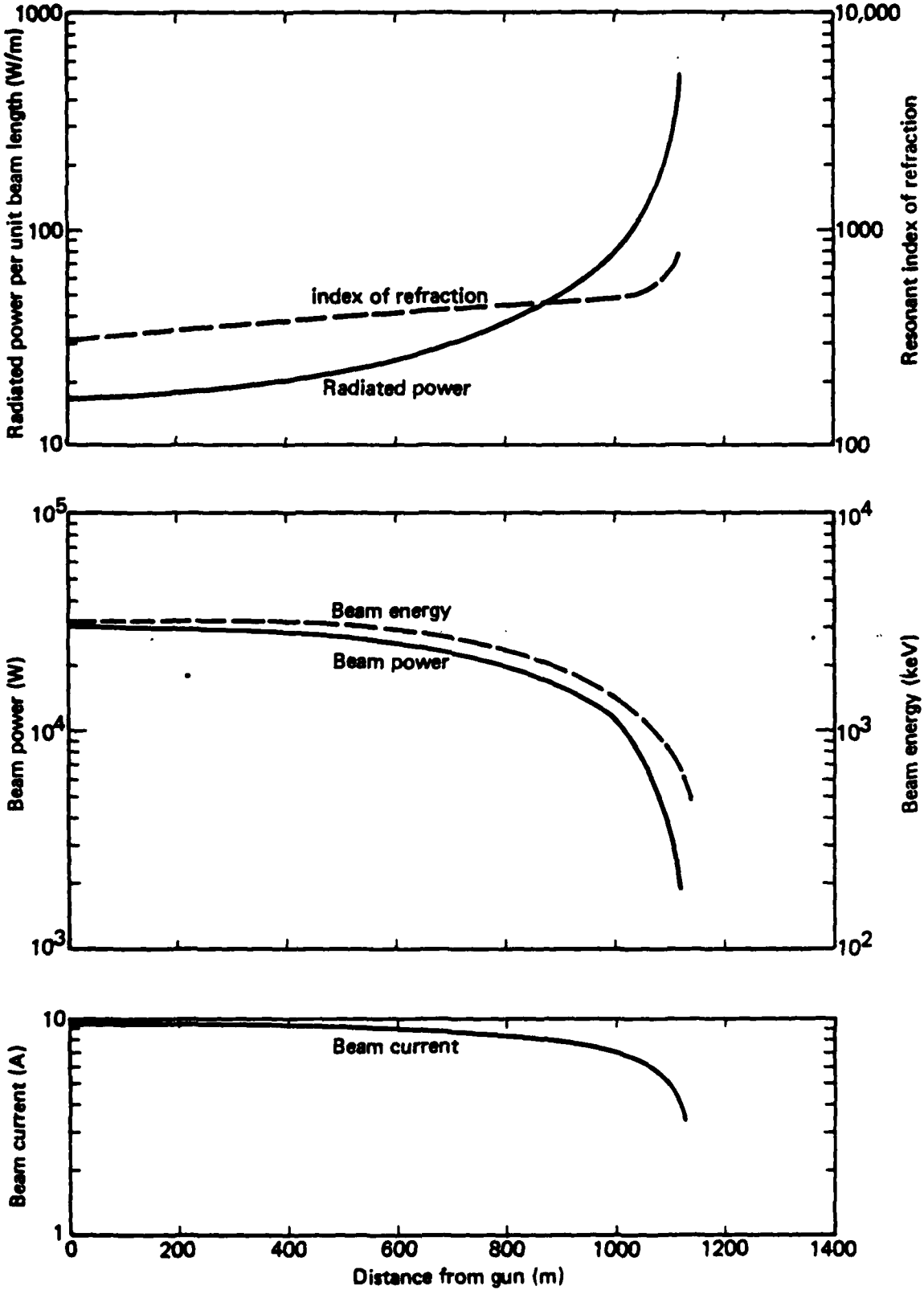

Figure 6. Effects of radiation energy loss: 40 kHz modulation frequency; 3 keV beam energy; 30 kW beam; 400 km altitude.

at least for this example, the direction of the radiation is unaffected. The propagation is affected, however, because the resonant index of refraction increases fivefold as the beam slows, the largest change occurring at low beam velocities.

We again emphasize the need for a full-fledged nonlinear treatment to accurately determine the extent and effects of beam slowdown.

V. CONCEPT VALIDATION EXPERIMENT

In Sec. IV we showed that a 1 keV beam will radiate several kilowatts into the Cerenkov mode, provided the frequency exceeds a few kilohertz and the beam retains its coherence for at least tens of meters. A 10 keV beam also radiates well in some cases, but would have to retain coherence over distances of hundreds to thousands of meters. As pointed out in Sec. II, beams in space have apparently traveled greater distances--although not necessarily at the energies and altitudes considered here. The limitations of the linear theory notwithstanding, those results indicate it might well be feasible to radiate a kilowatt or more from a modulated electron beam in space. According to Sec. III, that amount of radiation will be detectable at the ground, provided detection bandwidths less than about 100 Hz are achieved by coherently stacking the output of tens to hundreds of beam pulses. The necessary pulse stability appears achievable with present technology.

We conclude, therefore, that an experiment to modulate an electron beam in the ionosphere and detect the radiation on the ground has a good chance of success, provided the parameters are properly selected. In this section, we discuss the choice of parameters, outline in broad terms a concept validation experiment, and point out some additional theoretical work that is needed.

CHOICE OF PARAMETERS

Combinations of beam energy and modulation frequency for which there is no predicted radiation should be avoided. Figures 2 and 3 show those combinations as blank forbidden regions, which depend on altitude and, as shown in [7], vary diurnally. Initial experiments should be conducted at night, because of the relatively low ionospheric absorption and atmospheric noise. Reference [7] also shows that, for constant beam energy, the radiated power increases as the beam power increases; the beam power should therefore be maximized.

Figures 2 and 3 show that, for constant beam power, lowering the beam energy increases the radiation per unit length p. The current cannot be increased without limit simply by lowering the energy (voltage), however, because space charge causes current and voltage to be related through

$$\text{perveance} = I_m/V^{1.5} , \tag{10}$$

where I_m is the maximum current that can be extracted at voltage V. The perveance is determined by a gun's geometry.

There is, therefore, a trade-off: low energies (voltages) and high currents give the maximum radiation efficiencies, but require a high perveance and, hence, a large electron gun. A good compromise is reached by noting that a beam has only a given power--say 5 kW--that can be radiated, and that it is not necessary to maximize p (in watts per meter) to achieve that radiated power. Instead, it is necessary only that p be large enough for the radiation to occur before the beam is disrupted by processes discussed in Sec. IV. If we choose the voltage low enough that p is 100 W/m, for example, the 30 kW beam will radiate 5 kW in 50 m--a short distance. Nothing would be gained by lowering the voltage still further, causing the 5 kW radiation to occur in a distance shorter than 50 m; and something would be lost in increased electron-gun size and expense.

We therefore recommend using the highest voltage for which p is adequate; p = 100 W/m seems a reasonable criterion. Figures 2 and 3 show that, depending on altitude and frequency, that value for p can be achieved by choosing E between 1 and 10 keV. Higher values cause the beam to radiate too slowly; lower values cause the beam to radiate unnecessarily fast.

We next comment on the choice of altitude. Comparison of Fig. 2 with Fig. 3 shows that lower altitudes permit somewhat greater beam energies, which, as just discussed, have the advantage of reducing the required gun perveance. Table 3 shows high energies greatly extend the beam-plasma discharge length. Specifically, an energy on the order of

10 keV will cause adequate radiation at 200 km altitude, but not at 400 km. However, energies of about 1 keV will give good results throughout the 200- to 400-km altitude range. Placing the beam at a low altitude shortens the propagation path, hence increasing the ground-level signal.

In summary, available data is not sufficient to dictate a preferred altitude, but 200 km seems a somewhat better choice than 400 km.

BEAM-TO-GROUND TRANSMISSION EXPERIMENT

Figure 7 diagrams a possible configuration for a transmission experiment. Although the figure shows the electron gun on a shuttle, it might also be carried on a rocket. The relative merits of the two vehicles are discussed below.

The precise value of pitch angle is not important, but 45 deg is a good choice that allows for the possibility of cyclotron as well as Cerenkov emission. The analysis in [7] shows that the strongest radiated waves above a few kilohertz are backward waves that propagate nearly along the geomagnetic field, but in the opposite sense as the beam. Thus, for an upward-directed beam, as shown in Fig. 7, most radiated energy will propagate toward the ground. Some forward radiation also occurs, however, so some trials with the beam directed toward the ground should be included.

Basic Experiment

The main goal of the experiment is to detect radiation on the ground, so ground-based receivers are the most important instrumentation. One such receiver should be located near the end of the field line that guides the beam, because analysis in [7] shows the radiation is usually emitted on a cone whose axis is along the geomagnetic field; and low-frequency waves are often guided by the field. A second receiver should be located near the edge of the main footprint, whose size is not known and needs to be calculated. For now, we rely on data for whistlers and VLF emissions, which have footprints on the

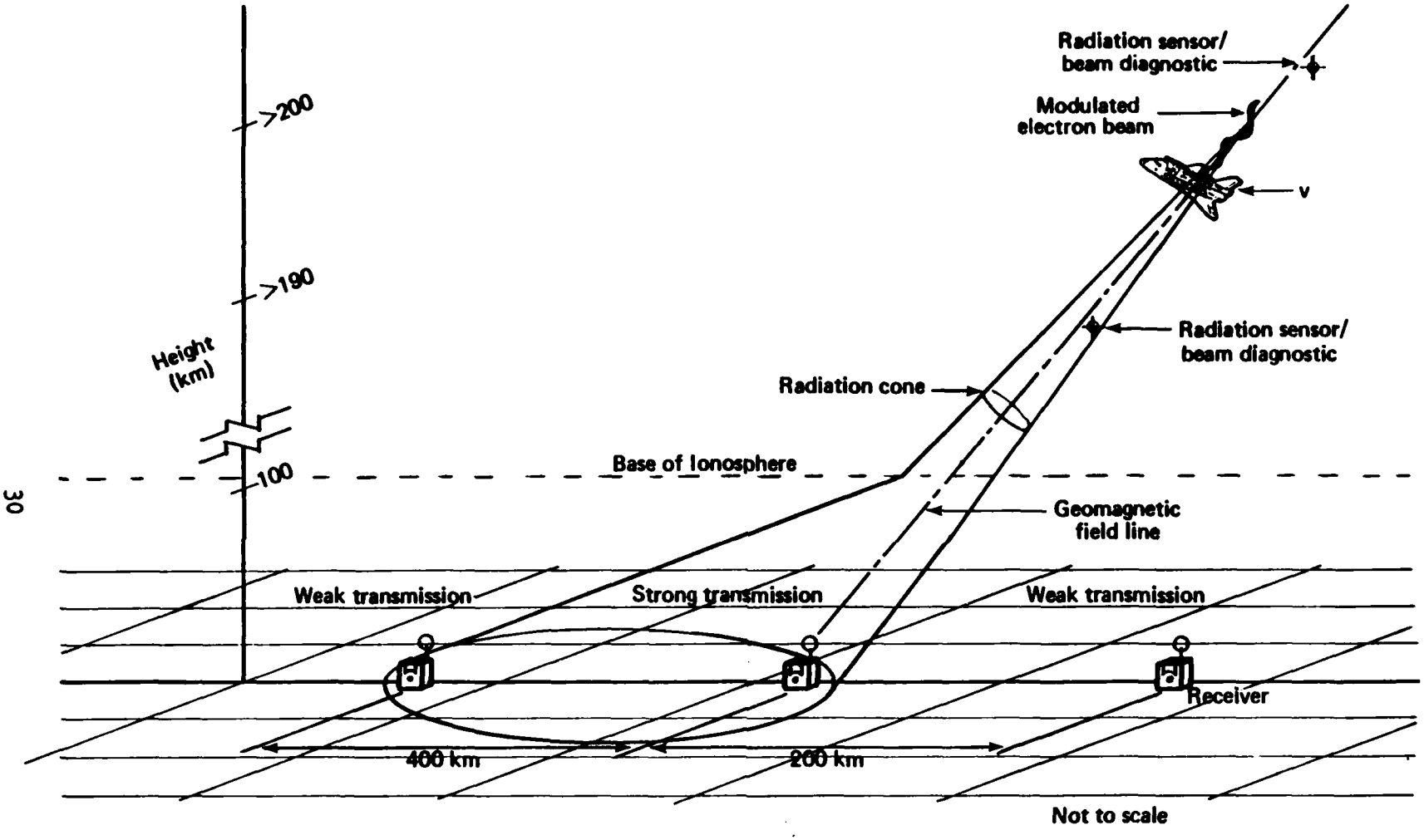

Figure 7. Schematic of concept validation experiment.

order of many hundreds of kilometers [23]. A third receiver should be located directly below the beam, thereby minimizing the transmission range. That configuration, shown schematically in Fig. 7, measures the magnitude of the signal and gives some information on ground coverage. If the electron gun is shuttle-borne, the footprint will sweep past all three receivers, giving additional data on geographic coverage.

Detection of energy that reaches the ground is the main goal, but it is also important to determine how effectively the beam couples electromagnetic energy to the ionosphere and how well the energy propagates. Such issues are best resolved with diagnostic packages located near enough to the beam to ensure detection of any energy radiated, but far enough away--perhaps several wavelengths--to be in the radiation field. Table 3 shows that these ionospheric far-field receivers should be separated about a kilometer from the beam. Figure 7 depicts two such receivers, one down and one up the field line. When the beam is directed upward, the lower one serves as a far-field receiver, and the upper one as a near-field beam diagnostic. When the beam is directed downward, the sensor roles are reversed.

OPTIONAL INSTRUMENTATION

The experiment described above is complete, relatively austere, and if successful, would demonstrate the feasibility of using virtual antennas to send low-frequency signals from space to the ground. There is, however, the risk that results would be difficult to interpret. It would be more satisfying, although more expensive, to instrument the experiment so that meaningful posttest analyses could be made--even if radiation is not detected on the ground. The above experiment makes no provision to monitor the environment immediately around the beam, or the state of the beam itself.

Figure 8 shows four categories of measurements that cover aspects from injection of the beam to reception on the ground. Measurements in the first category address the behavior of the electron beam. They monitor the beam current, its energy, the modulation frequency, and the degree of coherence as the beam leaves the vicinity of the injec-

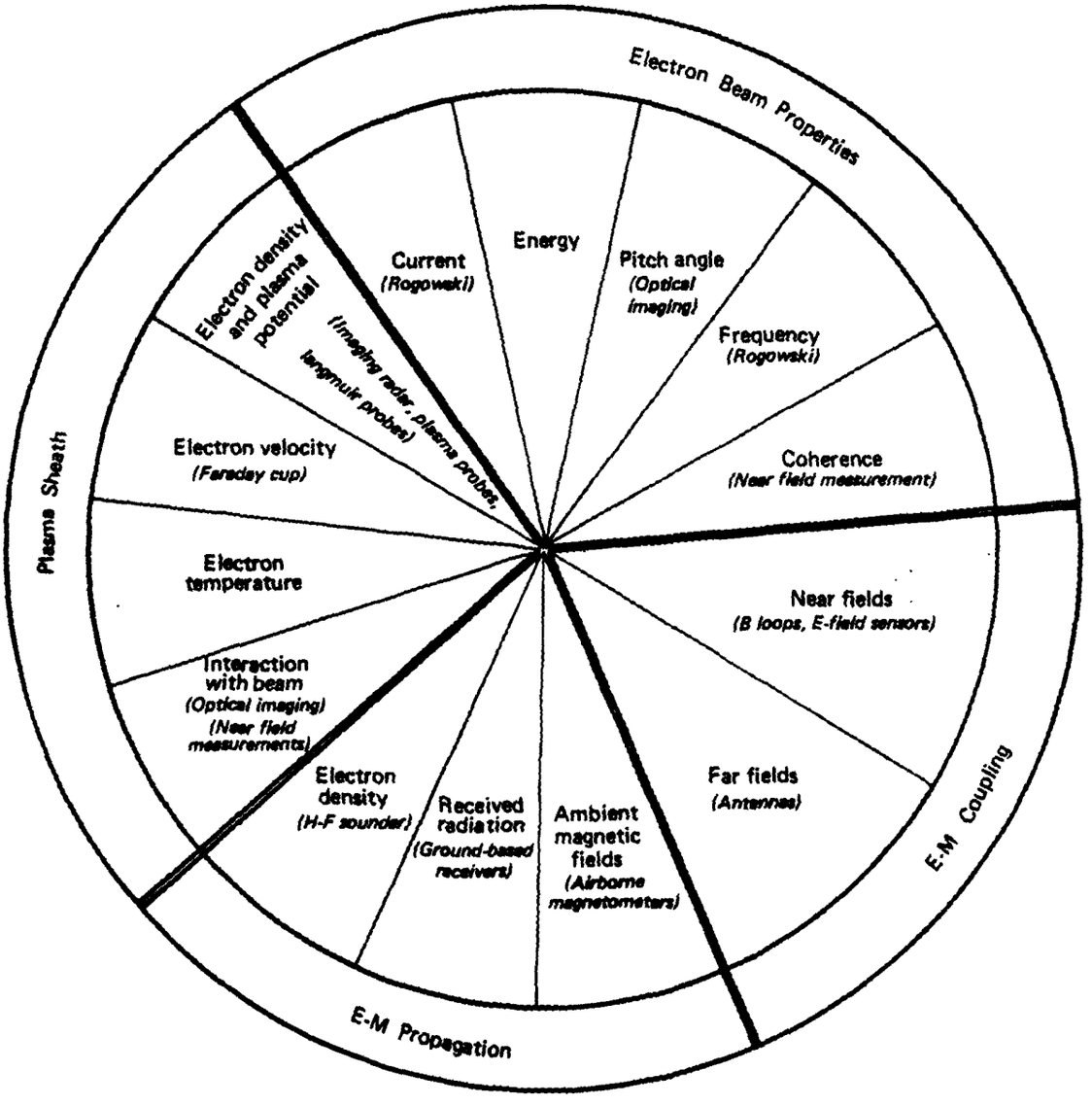

Figure 8. Categories of subsidiary diagnostic measurements.

tion gun. Those measurements ascertain whether the beam is emitted as intended, and how far from the gun it maintains coherence.

The diagnostic instrumentation is for the most part well understood. The initial beam parameters are controlled by gun design. The beam current is monitored by a Rogowski coil that surrounds the beam at the emitter. The coherence of the beam is somewhat harder to characterize. Current monitors on the ionospheric far-field platforms, discussed above and shown in Fig. 7 might suffice, but more work is needed on that aspect.

The second category characterizes the properties of the ionization sheath around the rocket and beam. These measurements probe the extent and nature of the plasma enhancement in the region where electromagnetic energy is being coupled to the plasma. Diagnostics include the electron density, the electron temperature, and the distribution and magnitude of return currents.

The ionization sheath around the beam may be monitored optically and by imaging radar. Ground-based and remotely deployed radars have been used in previous experiments to characterize the extent of the beam and the size of the sheath. The return currents are customarily monitored by Faraday cups and particle spectrometers placed at various locations on the spacecraft.

The third category of measurements probes the coupling of electromagnetic energy to the ionospheric plasma. Electric and magnetic field strengths in the near- and far-field regions should be monitored. Near-field measurements must be made within a few tens or hundreds of meters of the beam (see Table 3). Far-field measurements are discussed above.

The fourth measurement category addresses electromagnetic propagation. The most important measurement is of the electromagnetic fields at ground stations; an austere set of ground receivers is discussed above. Additional stations would, of course, help to define the size and shape of the footprint. In addition, a sounder could determine plasma frequency profiles in the propagation region. That information would allow detailed comparison of the received radiation

with predictions. Otherwise, propagation estimates must be based on nominal ionospheric models.

Rocket-borne and Shuttle-borne Experiments

The electron gun could be carried aloft by the space shuttle or by a rocket. Each platform has advantages and limitations. The main difference is that the shuttle would fly an extended mission, whereas a rocket would fly a brief mission, albeit over a range of altitudes.

If the shuttle is used, a great deal of data could be collected on one mission: trials could be made at several geomagnetic latitudes and times of day, and cooperating receivers could gather data worldwide. The shuttle can carry heavy payloads, including diagnostic packages. However, shuttle experiments are expensive, difficult to schedule, and must be compatible with other experiments carried on the same mission.

The beam and return current physics on the shuttle differs from a rocket, because only a small percentage of the shuttle exterior is metallic and grounded to the gun. The shuttle could therefore charge to a higher potential than a rocket and impede the injection of high electron currents. The SEPAC experiments showed that emission of a neutral gas or plasma during beam firing caused a high return current, which reduced shuttle charging [24], but the effect of such a modified plasma environment on radiation coupling is unknown. Neutral gas injection may not, therefore, be desirable on all shots.

The SEPAC experiments also showed that spacecraft charging depended strongly on whether or not the conductive segments of the shuttle were inside the wake [25]. When inside, the spacecraft charged to the gun potential; when outside, charging was limited to a few tens of volts. That effect was presumably due to the difference in plasma density inside and outside the wake. The effect of the wake on the beam's radiation is not known and should be investigated prior to a shuttle-borne experiment.

A rocket experiment is inexpensive and, being dedicated, free from the logistical constraints peculiar to shuttle experiments. If enough

power is available to drive the gun throughout the entire trajectory in the ionosphere, radiation could be attempted at several altitudes. A rocket can be launched from any facility that has appropriate airspace clearance and is not subject to the launch and orbital constraints of the shuttle. The rocket's main disadvantage is limited battery life and flight time, which require the mission to be short--6 to 10 min. A rocket experiment is therefore a "one-shot deal"; additional trials require additional launches.

In summary, initial experiments should probably be carried on inexpensive easily scheduled rockets. If those experiments are successful, shuttle experiments would be warranted.

UNRESOLVED THEORETICAL ISSUES

The theory of Harker and Banks [4], used in the present report, is the best available and gives encouraging results. Nonetheless, that theory makes several idealizations that must be relaxed before the results can be considered conclusive.

It is generally agreed (see Lavergnat and Lehner [26], for example) that the main shortcoming of existing theories is their neglect of the beam's collective fields on the trajectories of the electrons in the beam. Because of that neglect, those theories give the paradoxical result that a beam can radiate its entire energy without slowing down. Unfortunately, that lack of self-consistency is most pronounced precisely when the theories give the most interesting results--namely, when they predict the strongest radiation. Section IV gives a heuristic treatment of beam slowdown, but a nonlinear self-consistent theory is needed.

Available theories all assume the beam passes through, and radiates into, the ambient ionosphere. Actually, as mentioned throughout the present report, the beam and the host vehicle will modify the surrounding ionosphere substantially. The effect of those modifications on the radiation should be assessed.

Table 3 shows that the calculated radiation lengths are sometimes so short that they cast doubt on the assumption that the beam is long,

filamentary, and collimated. The theory should be extended to beams that are not much longer than their own diameter, and which have an angular divergence of several degrees.

Finally, a propagation analysis is needed to calculate the footprint of the radiation on the ground. That analysis will show, for example, where receivers should be placed to have the highest probability of detecting the radiation. The placements shown in Fig. 7 are rough empirical estimates, and subject to considerable uncertainty. An accurate theory requires calculation of the excitation of the earth-ionosphere waveguide.

REFERENCES

1. Bearce, L. S., Proceedings of the Conference on Antennas and Transionospheric Propagation as Related to ELF/VLF Downlink Satellite Communications, Naval Research Laboratory, NRL Report 7462, 27 November 1972.

2. Grossi, M. D., "New Technology for ELF Radiators: Review of Airborne, Rocket-borne, and Spaceborne Antennas," presented at AGARD 29th Symposium on Medium, Long, and Very Long Wave Propagation (at Frequencies less than 3000 kHz), Brussels, Belgium, AGARD CP-305, Paper 41, February 1982.

3. Harker, K. J., and P. M. Banks, "Radiation from Pulsed Electron Beams in Space Plasmas," Radio Sci., Vol. 19, No. 2, March-April 1983, pp. 454-470.

4. Harker, K. J., and P. M. Banks, "Radiation from Long Pulse Train Electron Beams in Space Plasmas," submitted to Planet. Space Sci., 1985 (to be published).

5. Lavergnat, J., T. Lehner, and G. Matthieussent, "Coherent Spontaneous Emission from a Modulated Beam Injected in a Magnetic Plasma," Phys. Fluids, 27(7), July , 1984, pp. 1632-1639.

6. Ohnuki, S., and S. Adachi, "Radiation of Electromagnetic Waves from an Electron Beam Antenna in the Ionosphere," Radio Sci., Vol. 19, No. 3, May-June 1984, pp. 925-929.

7. Johnson, L. E., Experiments in Long-Wave Communication Using Modulated Electron Beam Antennas: A Parameter Study, Pacific-Sierra Research Corporation, Report 513, January 1985.

8. Ellis, B. R. A., "Low Frequency Radio Emission from Aurorae," J. Atmos. Terr. Phys. 10, 1957, pp. 302-306.

9. Winkler, J. R., "The Application of Artificial Electron Beams to Magnetospheric Research," Rev. Geophys. Space Phys., Vol. 18, No. 3, August 1980, pp. 659-682.

10. Cartwright, D. G., and P. G. Kellogg, "Observations of Radiation From an Electron Beam Artificially Injected Ionosphere", J. Geophys. Res., Vol. 79, No. 10, 1 April 1974, pp. 1439-1457.

11. Holzworth, R. H., and H. C. Koons, "VLF Emissions From a Modulated Electron Beam in the Auroral Ionosphere," J. Geophys. Res., Vol. 86, No. A2, 1 February 1981, pp. 853-857.

12. Shawhan, S. D., and G. B. Murphy, "Wave Emissions from DC and Modulated Electron Beams on STS 3," Radio Sci., Vol. 19, No. 2, March-April 1984, pp. 471-486.

13. Taylor, W. W. L., et al., "Wave-Particle Interactions Induced by SEPAC on Spacelab-1: Wave Observations," Radio Sci., Vol 20, No. 3, May-June 1985, pp. 486-498.

14. Booker, H. G., C. M. Crain, and E. C. Field, Transmission of Electromagnetic Waves through Normal and Disturbed Ionospheres, The Rand Corporation, Santa Monica, California, November 1970.

15. Watt, A. D., VLF Radio Engineering, Pergamon Press, London, England, 1967.

16. Watt, A. D., and E. L. Maxwell, "Measured Statistical Characteristics of VLF Atmospheric Radio Noise," Proc. IRE, January 1957, pp. 55-62.

17. Evans, J. E., and A. S. Griffiths, "Design of a Sanguine Noise Processor Based Upon World-Wide Extremely Low Frequency (ELF) Recordings," IEEE Transactions on Communications, Vol. COM-22, No. 4, April 1974.

18. Harker, K. J., and P. M. Banks, "Near Fields in the Vicinity of Pulse Electron Beams in Space," STAR Laboratory, Stanford University, paper presented at XXIst General Assembly of URSI, Florence, Italy, 28 August-5 September 1984.

19. Etcheto, J., and R. Gendrin, "About the Possibility of VLF Cerenko Emission in the Ionosphere by Artificial Electron Beams," Planet. Space Sci., Vol. 18, 1970, pp. 777-784.

20. Karpman, V. I., "Cerenkov Radiation and the Front Structure of a Beam Injected into the Ionosphere," Planet. Space Sci., Vol. 22, 1974, pp. 1597-1610.

21. Szuszczewicz, E. P., "Laboratory Simulations of Controlled Energetic Electron-Beam-Plasma Interactions in Space," AIAA J., Vol. 21, No. 10, October 1983, pp. 1374-1381.

22. Sasaki, S., et al., "Ignition of Beam Plasma Discharge Observed in the Electron Beam Experiment in Space," submitted to Geophys. Res. Let., April 1985 (to be published).

23. Helliwell, R. A., Whistlers and Related Ionospheric Phenomena, Stanford University Press, Stanford, California, 1965.

24. Sasaki, S., et al., "Effect of Plasma Injection on the Electrical Charging of a Vehicle Emitting an Electron Beam Observed in SEPAC SPACELAB-1 Experiment," submitted to AIAA J. Spacecraft Rockets, May 1985 (to be published).

25. Sasaki, S., et al., "Vehicle Charging Observed in SEPAC SPACELAB-1 Experiment," submitted to AIAA Journal of Spacecraft and Rockets, December 1984 (to be published).

26. Lavergnat, J., and T. Lehner, "Low Frequency Radiation Characteristics of a Modulated Electron Beam Immersed in a Magnetized Plasma," IEEE Trans. Antennas Propag., Vol. AP-32, No. 2, February, 1984.

MISSION
of
Rome Air Development Center

RADC plans and executes research, development, test and selected acquisition programs in support of Command, Control, Communications and Intelligence (C^3I) activities. Technical and engineering support within areas of competence is provided to ESD Program Offices (POs) and other ESD elements to perform effective acquisition of C^3I systems. The areas of technical competence include communications, command and control, battle management, information processing, surveillance sensors, intelligence data collection and handling, solid state sciences, electromagnetics, and propagation, and electronic, maintainability, and compatibility.